Distributed 3D Aspect Ratios of Toner

Kevin Lofftus, Eastman Kodak Company, Rochester NY/USA

Abstract

Two-dimensional shape analysis of toner may be extended to three dimensions by combining shape information from typical image analysis of oriented toner with information from instruments that measure toner volume such as the Coulter Multisizer. A mean aspect ratio for the hidden dimension perpendicular to the plane of the image can be estimated by assuming a model shape such as an ellipsoid. Furthermore, if the shape is independent of the size, a relationship between the aspect ratio of the hidden dimension and the aspect ratio of the visible dimensions may be developed. Shape is independent of size when brittle fracture dominates the grinding process in melt-pulverized toners (MPT) and is independent by design in the limited coalescence manufacturing method used to make chemically prepared toner (CPT). The relationship between the different aspect ratios is useful to distinguish toners that have flat disk-like particles from toners with spherical particles within a broader distribution of shapes that result in different performance in the electrophotographic process.

Introduction

Toner shape influences toner powder flow, bottle fill, developer flow, transfer efficiencies, and cleaning properties in electrophotographic print engines. Control of particle shape is an advantage of chemically prepared toner (CPT) manufacturing methods. Image analysis can only characterize two dimensions of a particle. It was shown [1] that orientation effects of some image analyzers may be used in combination with other size measurements to characterize the shape in three dimensions. A method to determine the overall average aspect ratio of a CPT perpendicular to the image plane of an image analyzer where the particles are oriented by flow was demonstrated. It has been found that the distribution of this aspect ratio is needed to characterize flow and cleaning properties of a CPT. A method to determine the conditional distribution with respect to semi-major aspect ratio and estimate of this marginal distribution is presented.

Background

An ellipse is a fair description of images of oriented CPT made by the evaporative limited coalescence (ELC) manufacturing process [2]. In the ELC process, spherical droplets containing solvent, polymer, colorant, and other addenda are stabilized in water with a colloid resulting in narrow log-normal size distributions. By controlling the rearrangement of the colloidal stabilizer during the evaporation of the solvent, the shape of the CPT can be varied from spherical to a variety of highly folded shapes.

For an ellipse, the projected area A_p and circular equivalent diameter D_{CE} are related to the major axis a and to the (inverse) semi-minor aspect ratio R_b:

$$A_p = \pi D_{CE}^2 / 4 = \pi R_b a^2 / 4 . \quad (1)$$

Likewise, the volume of an ellipsoid V and spherical equivalent diameter DSE are related to the major axis a, the (inverse) semi-minor aspect ratio R_b, and the (inverse) minor aspect ratio R_c:

$$V = \pi D_{SE}^3 / 6 = \pi a^3 R_b R_c / 6 . \quad (2)$$

Eliminating the major axis a and solving for R_c, we have

$$R_c = \sqrt{R_b}\left(D_{SE} / F D_{CE}\right)^3 . \quad (3)$$

where F is the instrument cross calibration factor.

A highly spherical CPT of similar composition and size to the sample of interest may be used to determine F using Eq. (3) with aspect ratio values of one ($F = D_{SE,Cal} / D_{CE,Cal}$). It was shown previously [1] that the difference between the D_{CE} measured on a Sysmex FPIA3000 and D_{SE} measured on a Coulter Multisizer was dependent upon size and color. The size dependence of F for imaged particles is complex due to forward scattering modulating the light collected by the imaging optics. The Sysmex FPIA3000 software has a built-in calibration method to convert A_p to D_{CE}. The 20X objective for the Sysmex FPIA3000 imaging optics has an aperture with an F-stop setting. It was found that the F-stop had been moved from the factory setting and gave incorrect values of D_{CE} for some sizes. When the aperture F-stop was set correctly, the size dependence of F was eliminated and there was no color dependence except for CPT's with fluorescent pigments.

It was found that CPT's with fluorescent pigments interacted with particle shape to give low D_{CE}'s. Morphology-dependant resonance modes in spherical particles such as the so-called whispering gallery mode [3] can greatly increase the path length of near-tangent light resulting in increased off-peak adsorption and greater fluorescence [4] and lasing [5, 6] near the periphery of the sphere. The fluorescent light lowers the contrast of the particle image edge and edge detection algorithms underestimate the particle size. The reduction in image size for irregular toners does not occur because few resonance modes can exist in nonspherical particles.

Estimation for R_c is sensitive to the value of F due to the cubic power in Eq. (3). Changes in focus on the Sysmex FPIA3000 and Coulter Multisizer performance necessitates evaluating F frequently. Several methods of determining the most reliable estimates of $D_{SE,Cal}$ and $D_{CE,Cal}$ were investigated. The calibration may be affected by differences in fines sensitivity, fines artifacts, and aggregation rates [6, 7] between the FPIA3000 and Coulter Multisizer. These differences may be minimized by using data limited to the distribution mode. Finding the quartic root of derivative of the least-squares fit to a fifth-order polynomial for data at least one half of the mode height was found to work well for symmetric log-normal distributions produced by ELC but not for asymmetric distributions of melt-pulverized toners (MPT). Taking the average for the data of at least one third of the mode height was found to be more robust to both mode shape and channel-to-channel noise.

Information about the distribution of the minor aspect ratio is hidden within the joint size and semi-major aspect ratio distribution. By finding the R_c for each R_b using Eq. (3), the conditional distribution of R_c given R_b may be estimated if the shape is independent of size. Likewise, the conditional size distribution for Log(D_{CE}) given R_b may be evaluated to test the independence of shape and size and verify that the evaporation process is in control. For CPT's formed by the ELC process, the size distribution is determined by the limited coalescence process and the shape is determined by the evaporation process.

When there is no variation in R_c the variation in D_{CE} is equal to that in D_{SE}. By applying a mass balance to Eq. (3) over a size distribution and assuming size and shape independence, one can derive an expression for the minimum independent variation in R_c:

$$\sigma^2_{\log(R_c)} = 9\left(\sigma^2_{\log(D_{SE})} - \sigma^2_{\log(D_{CE})}\right). \quad (4)$$

Particles with more spherical character may be formed by extreme conditions in the evaporation process. These spherical particles may be either smaller or larger than those formed in the coalescence stage and evaluation of Eq. (4) can lead to negative estimates of variance in R_c.

Materials and Methods

Pilot scale cyan CPT's were evaluated for size and shape distribution and correlated to performance in Kodak NexPress digital production color presses. The current MPT cyan toner from Kodak was used as a control. To characterize shape, a dispersion of CPT at 0.200% in water using a mixture of ionic and nonionic surfactants [7] was measured on a FPIA3000 and a Multisizer 3. The joint distribution of D_{CE} and R_b from the FPIA3000 was analyzed using 226 D_{CE} bins from 1 to 25 μm on a log scale and 140 R_b bins from 0.3 to 1. The pulse data were collected for Multisizer 3 and reprocessed to remove the recount artifact from the fines [8]. Count rates were reduced to a point where few coincidence events occurred for both instruments.

Focus of the Sysmex FPIA3000 was maintained to ±0.02 μm using a 1.9 μm polystyrene latex bead (Duke Scientific Inc. 5200B). It was found that constructive interference from refracted and diffracted light coincides with the particle edge for this size particle when the separation between the cell and the 20X objective is too great. The result enhanced edge sharpness and a measured size of 1.80 μm. The autofocus routine selects a cell position that results in the enhanced edge sharpness and it was necessary to focus using a 1.03 μm polystyrene latex bead (Duke Scientific Inc. 5100A).

It was found helpful for texture characterization [9] to limit the size of data processed to reduce the impact on mass balances due to differences in fines sensitivity and coarse particle aggregation. Limiting the size for shape analysis has little impact on the conditional R_c distribution for the conditions described above. Some improvement was seen for evaluating the independence of shape and size and the limiting procedure [9] was applied for all samples.

The conditional R_c was evaluated for R_b bins with 10 or more particles from which the mean, standard deviation, and trend with respect to R_b were calculated. As a test for size and shape independence, the weighted average of the log-normal widths expressed as variances in Log(D_{CE}) at each R_b were computed and used to evaluate Eq. (4). Also, the independences were evaluated graphically by comparing variances at each R_b for D_{CE} with that for D_{SE} using 90% confidence intervals for a χ^2 distribution.

Results

Table 1 shows the results of various pilot scale CPT's demonstrating ranges of performance in Kodak NexPress printers. Generally there was no trend in R_c with R_b for ELC processes giving the desired shape. Evaluating R_b alone (Figure 1a), one would predict that the CPT labeled Oblate would perform similarly to the CPT labeled Spherical, resulting in low developer flows and blade cleaning failures. However the conditional R_c distribution for the oblate CPT was similar to the CPT and MPT that had acceptable performances (Figure 1b). The estimated marginal R_c distribution was narrower with a higher mean R_c. Performance of the oblate CPT was in fact opposite that for the spherical CPT resulting in high to flow adjustment sensitivities.

Table 1: Selected CPT Shape Characteristics

	R_b	σR_b	R_c	σR_c	dR_b/dR_c	$\sigma^2_{Log(Rc)}$
MPT	0.797	0.108	0.562	0.039	0.033	0.0086
CPT	0.836	0.094	0.609	0.043	0.138	0.0031
Spherical	0.912	0.071	0.823	0.128	1.495	-0.0012
Oblate	0.886	0.068	0.686	0.035	0.379	0.0006
Broad R_c	0.853	0.107	0.697	0.111	0.898	0.0027
Mixed	0.768	0.120	0.599	0.033	0.222	0.0059
Variant 1	0.800	0.111	0.585	0.067	0.443	-0.0029
Variant 2	0.852	0.091	0.573	0.034	0.145	-0.0123

It is assumed in Eq. (3) that the CPT has a convex particle shape. The computed R_c is lower than the physical dimension of a particle with significant concavities. Concavities in MPT are shallow and have little impact on R_c. On the other hand, significant volume may be obtained for highly shaped CPT's by folding during evaporation of the original oil phase spherical surface. This original surface may be greater than three times that of the spherical CPT when no shape control is applied (Figure 2). The manner of curling may produce CPT's of mixed oblate and prolate character with broad R_b and R_c marginal distributions but narrow conditional R_c (Mixed in Table 1 and Figure 3).

Shape distributions may be affected by extreme conditions during processing. Variations in shape without changes in the size distribution will result in broad R_c marginal distributions with increased trends with R_b in conditional distributions while the minimum independent variation in R_c would not be affected (Broad R_c in Table 1 and Figure 3). Process extremes that cause size changes after coalescence do not necessarily produce broad R_c marginal distributions but will generate trends in R_c with R_b and negative estimates for the minimum independent variation in R_c (Spherical and Variant 1 in Table 1 and Figures 1 and 3). Process extremes that modify the shape after evaporation will lead to negative estimates for the minimum variation in R_c while maintaining narrow R_c marginal distributions and low trends with R_b (Variant 2 in Table 1).

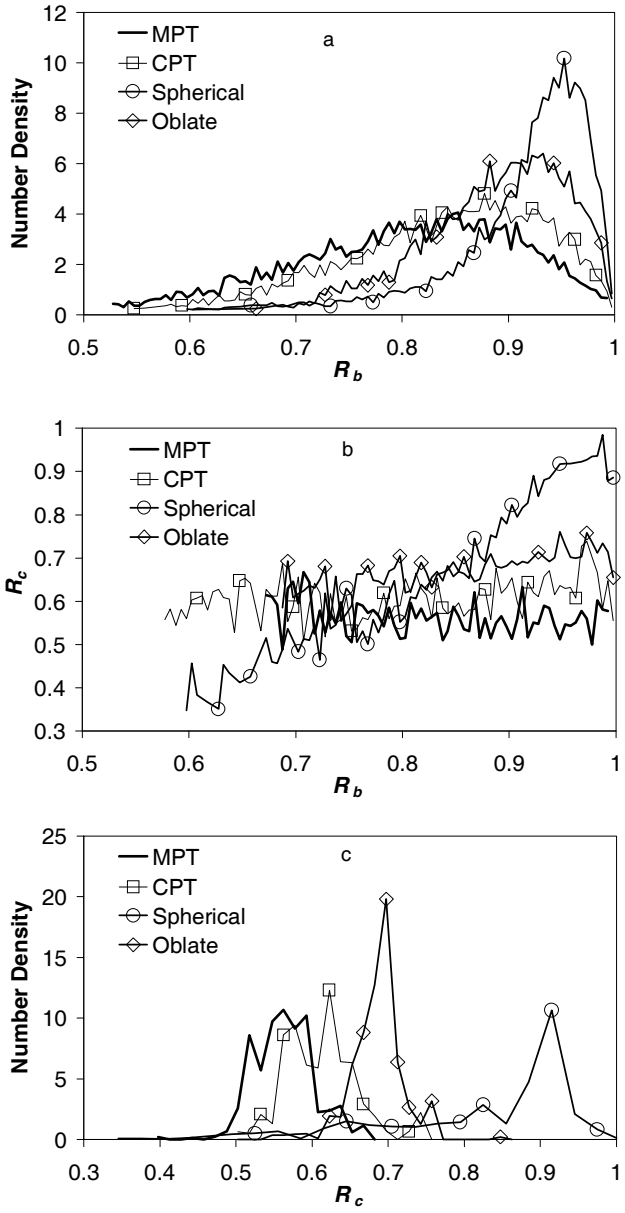

***Figure 1**. Comparison of three CPT's to MPT: a) marginal R_b distribution, b) conditions R_c distribution, and c) estimated marginal R_c.*

Widths of the R_c conditional distributions (σR_c in Table 1) are increased by the increased trends with R_b and by wider R_b marginal distributions (high σR_b in Table 1). Because R_c is not entirely independent of R_b, the width of the conditional R_c distribution represents the dependent variation in R_c. Some extreme conditions may lead to CPT's with lower dependent variation σR_c yet having negative values for the estimate of the minimum independent variation in R_c. A mixture of different shapes where the size distributions are different in either size or width will lead to broader Coulter Multisizer size (D_{SE}) distributions. The width of the conditional Sysmex size (D_{CE}) distribution as a function of R_b will show regions with greater variation in Log(D_{CE}) than Log(D_{SE}) and regions with less. Regions with greater variation in Log(D_{CE}) arise where the different shapes have the same R_b while regions with less have a single shape.

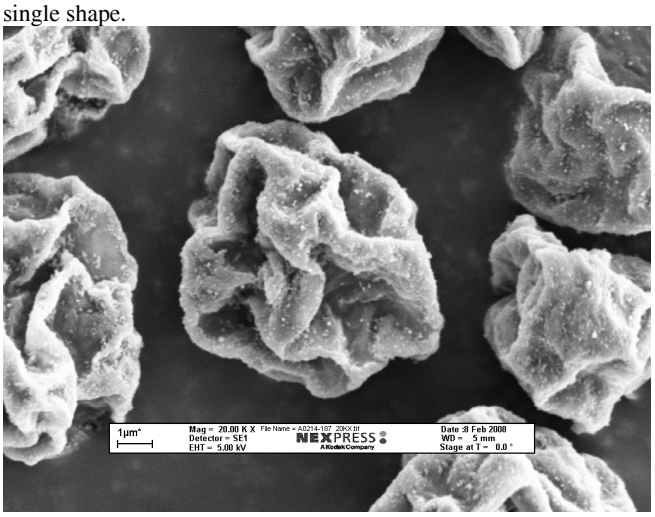

***Figure 2.** CPT with high degree of concavities leading to high independent variation in R_c of 0.015.*

A combination of spheres and oblate ellipsoids of different size or size distribution widths will result in conditional D_{CE} distributions that are wider then the D_{SE} distribution for higher R_b. Figure 4 shows one such CPT that exhibited developer flow problems due to a high content of spheres. In comparison, MPT's and CPT's that perform well have no change in the conditional variation of Log(D_{CE}) over the entire range of R_b (Figure 4).

Occasionally one finds a CPT where the variation in Log(D_{CE}) is less than that for Log(D_{SE}) over all R_b's. This implies that R_c has a variation not dependent upon R_b. The independent variation in R_c arises when the ellipsoid does not model the shape of the toner. The blocky nature of MPT's is not well modeled by ellipsoids and values for the independent variation ($\sigma^2_{\mathrm{Log}(Rc)}$) are about 0.009 (Table 1). Folding of an ELC CPT using shape control may give some blocky character but low values of $\sigma^2_{\mathrm{Log}(Rc)}$. High values of $\sigma^2_{\mathrm{Log}(Rc)}$ may be seen due to variation in the volume of the concavities such as those for the CPT in Figure 2 which has a $\sigma^2_{\mathrm{Log}(Rc)}$ value of 0.015. The cavity volume is not modeled by a solid ellipsoid and any variation in this volume without the corresponding change in D_{CE} will lead to increased values for $\sigma^2_{\mathrm{Log}(Rc)}$.

Conclusion

Image analysis shape and size distributions can be used in combination with Coulter Multisizer size distributions to characterize 3D shape distributions. The minor aspect ratio R_c may be characterized by the conditional distribution with respect to semi-major aspect ratio R_b and by an estimated marginal distribution when the shape is independent of size. The independence of shape and size may be tested by comparing the variation of the spherical equivalent diameter from a Coulter Multisizer to that for the Sysmex circularly equivalent diameter conditional upon R_b. Statistics and trends in these shape distributions can be correlated to performance in electrophotographic printing set requirements for the manufacturing of chemically prepared toners.

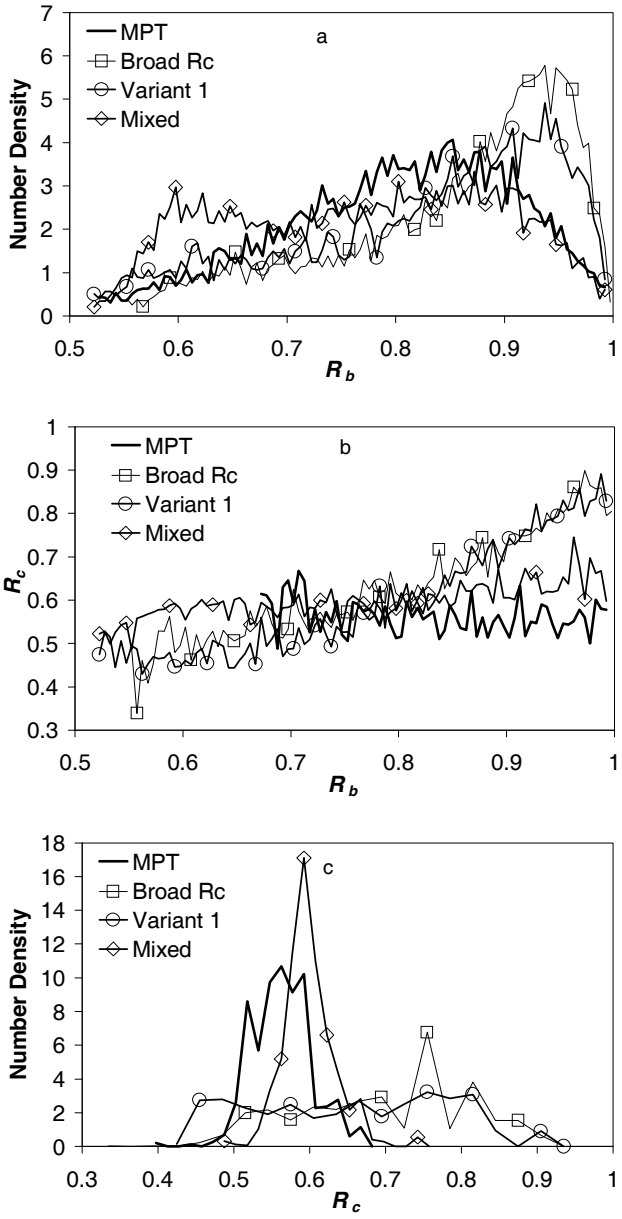

***Figure 3**. CPT's having unique shape characteristics: a) marginal R_b distribution, b) conditions R_c distribution, and c) estimated marginal R_c.*

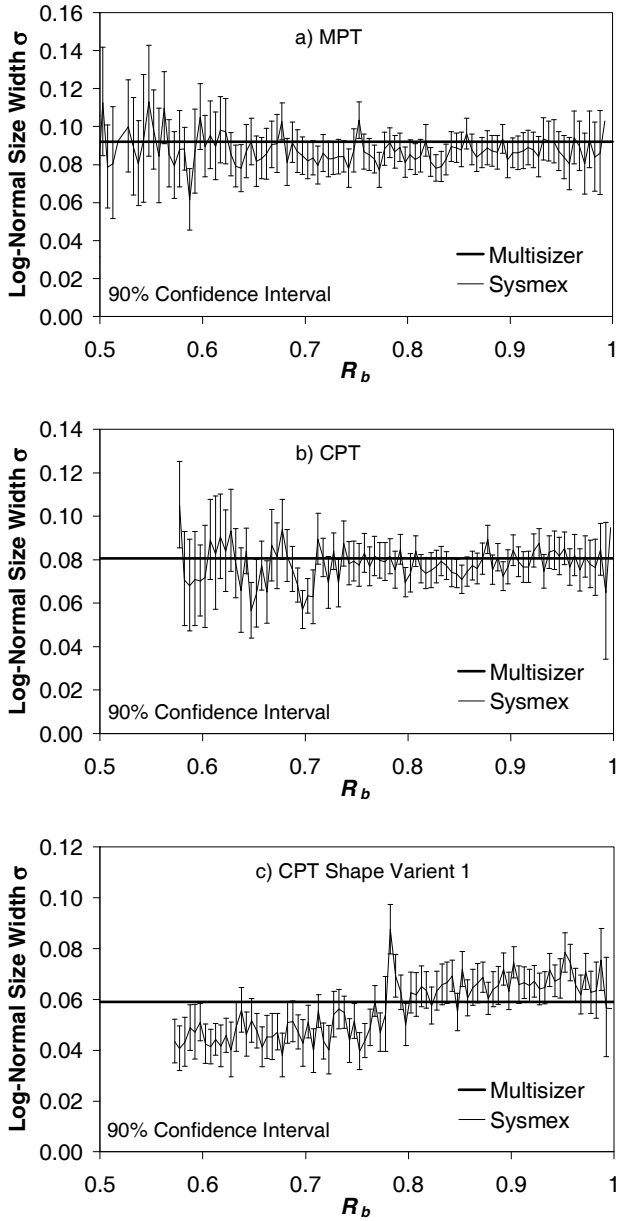

***Figure 4**. Graphical evaluation of shape and size independence for a) MPT, b) CPT with acceptable performance, and a CPT with both oblate and spherical shapes for $R_b > 0.78$ resulting in flow difficulties.*

References

[1] Lofftus, Extending Toner Shape Analysis to 3D, Proc. NIP23 (IS&T, Fairbanks, AL, 2007) pp. 209–212.

[2] Nair, Pierce, and Sreekumar, US Patent 4833060, 1989.

[3] Gorodetsky and Fomin, "Geometrical theory of whispering gallery modes," Selected Topics in Quantum Electronics, IEEE J. of, 12, pp. 33–39 (2006)

[4] Barnes, Whitten, and Ramsey, "Enhanced fluorescence yields through cavity", J. Opt. Soc. Am. B, 11, pp 1297–1304 (1994).

[5] Zhang et al., "Observation of whispering-gallery and directional resonant laser emission in ellipsoidal microcavities," J. Opt. Soc. Am. B, 23, pp 1793–1800 (2006).

[6] Schiro and Kwok, "Cavity-enhanced emission from a dye-coated micropshere," Optics Express, 12, pp. 2857–63 (2004)

[7] Lofftus, Improvements in Toner Fines Characterization, Proc. NIP21 (IS&T, Baltimore, MA, 2005) pp. 484–487.

[8] Lofftus, Time Discrimination of Coulter Recount Artifact, Proc. NIP22 (IS&T, Denver, CO, 2006) pp. 161–164.

[9] Lofftus, Texture Characterization of Chemically Prepared Toners, Proc. NIP24 (IS&T, Pittsburg, PA, 2008).

Author Biography

Kevin Lofftus received a B. S. in 1982 and an M. S. in 1984 for Mineral Process Engineering from Montana College of Mineral Science and Technology and a Ph. D. in 1989 from The University of California Berkeley for Mineral Processing with minors in Chemical Engineering and Statistics. He joined the Copy Products Division of Kodak in 1989 and is currently a Senior Research Scientist at Eastman Kodak Company